JOURNAL OF THEORETICAL AND APPLIED MECHANICS
55, 2, pp. 667-677, Warsaw 2017
DOI: 10.15632/jtam-pl.55.2.667

ROLE OF WAVE REVERBERATIONS IN EXIT VIBRATIONS OF PROJECTILES AND SHELLS

Radosław Trębiński
Military University of Technology, Faculty of Mechatronics and Aerospace, Warszawa, Poland
e-mail: rkt@wat.edu.pl

Carlucci *et al.* (2013) proposed a theoretical model describing exit vibrations of a shell launched by a gun. The model treats the shell as a system of a spring, damper and a rigid mass. In this paper, similar models describing vibrations of shells and monolithic projectiles are compared with some 1D models taking into account wave reverberations. The comparison proves that the models taking into account the wave motion, forecast similar amplitudes and frequencies of vibrations as discrete models. However, details of acceleration time courses differ considerably. The problem of the influence of the friction force between the shell wall and the filling is also discussed. The results of modelling serve as well for assessing if some projectile velocity oscillations detected by making use of the Doppler radar can be solely attributed to the exit vibrations.

Keywords: intermediate ballistics, projectile vibrations, wave reverberation

1. Introduction

Projectiles and shells moving inside a gun tube undergo compression. After leaving the muzzle, they experience a sudden drop of pressure acting on their base. This decompression causes vibrations of the projectiles and shells, which can be detrimental for the integrity of their inner structure. Ammunition designers take this into account by assuming that there is a step drop of the pressure from the muzzle pressure to the ambient pressure. However, recently some data became available enabling designers to take into account the continuous character of the pressure changes. On the basis of accelerometer records, Carlucci and Vega (2007) proposed an approximation of pressure changes by the exponential decay curve

$$p(t) = p_m \exp(-\beta t) = p_m \exp\Big(-\frac{t}{t_m}\Big) \tag{1.1}$$

Values of the muzzle pressure p_m and the coefficient β were published for a 155 mm cannon in Carlucci and Vega (2007) and Carlucci *et al.* (2013).

Some theoretical models were considered by Trębiński and Czyżewska (2015a,b), enabling calculation of pressure courses acting on the projectile in the intermediate period. On the basis of the results of calculations for a broad range of launching systems, an approximate formula was proposed for calculating the value of the coefficient β for a launching system of the caliber d

$$\beta = (0.74 + 0.24M_m)\frac{u_m}{d} \tag{1.2}$$

Values of the muzzle flow Mach number M_m and the muzzle velocity u_m can be determined on the basis of results of internal ballistics calculations.

In Carlucci *et al.* (2013), a model was proposed describing vibrations of a shell subjected to the action of a pressure pulse (1.1). The motion of the ogive of the shell was modeled in

the reference frame moving with the center of gravity of the shell. The ogive was treated as a rigid mass, whereas the wall of the shell was treated as a spring. Its inertia was taken into account by adding one third of its mass to the mass of the ogive. A damper was added in order to take into account damping of the vibrations. The model predicts a considerable magnitude of acceleration oscillations, which is in qualitative agreement with experimental observations. Considering accelerometers as vibrating systems showed very small influence of their inertia and rigidity on the courses of acceleration, except for the very beginning of the process.

The determined values of the period of vibrations of projectiles and shells as well as the characteristic time t_m in expression (1.1) are close to the values of the reverberation time of elastic waves moving in projectiles and shells. In such a case, one can expect that the results of modeling with the use of discrete models and models incorporating wave motion may differ considerably. This paper is devoted to analysis of the role of wave reverberations. The main objective of this analysis is to determine to which extent the amplitudes and frequencies of the exit vibrations of projectiles and shells forecasted by discrete models and models taking into account wave reverberations differ. Several 1D models of the wave motion in a projectile or a shell, when subjected to action of the pressure pulse described by (1.1), are considered. Conclusions concerning the potential influence of wave processes on the indications of accelerometers embedded in the projectiles and shells are formulated.

Doppler radar measurements of the velocity changes of a projectile leaving the muzzle of a 30 mm launching system, presented in Leciejewski *et al.* (2013), showed oscillations of the velocity value (Fig. 1). The question arose whether these oscillations can be attributed solely to the vibrations of the projectile. Finding the answer to this question was the secondary objective of the analysis presented in this paper.

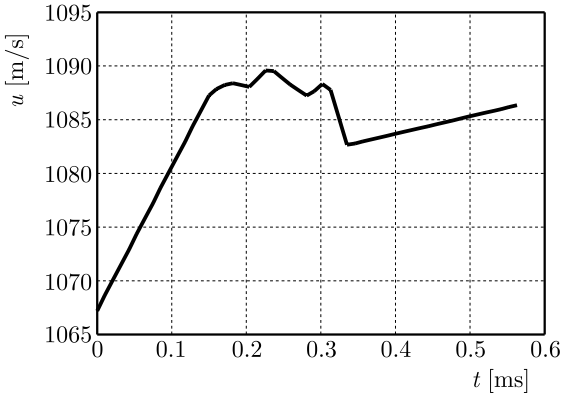

Fig. 1. Results of measurements of the projectile velocity changes outside the muzzle of a 30 mm launching system (Leciejewski *et al.*, 2013)

2. Models

2.1. Models of a monolithic projectile

The sense of physical models considered can be explained by referring to Fig. 2. In model 1, the projectile is considered as a system of two rigid masses m_1 and m_2 connected by a spring. The stiffness of the spring is determined as

$$k_s = \frac{AE}{l_0} \qquad A = \frac{\pi d^2}{4} \tag{2.1}$$

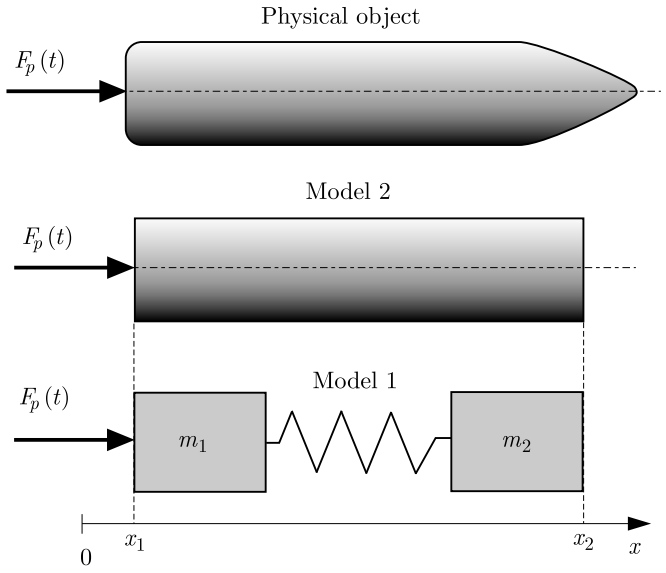

Fig. 2. Schemes of models 1 and 2

The mathematical model corresponding to physical model 1 is given by the following initial value problem

$$\begin{aligned} &m_1\frac{d^2x_1}{dt^2} - k_s(x_2 - x_1 - l_0) = Ap_m\mathrm{e}^{-\frac{t}{t_m}} \qquad m_2\frac{d^2x_2}{dt^2} + k_s(x_2 - x_1 - l_0) = 0 \\ &x_1(0) = 0 \qquad x_2(0) = l_0 - \frac{m_2Ap_m}{(m_1+m_2)k_s} \qquad \frac{dx_1}{dt}\Big|_{t=0} = \frac{dx_2}{dt}\Big|_{t=0} = u_m \end{aligned} \tag{2.2}$$

Dividing the first equation by m_1 and the second one by m_2 and summing up the equations, we obtain

$$\frac{d^2(x_2 - x_1)}{dt^2} + \Big(\frac{k_s}{m_1} + \frac{k_s}{m_2}\Big)(x_2 - x_1 - l_0) = -\frac{F_p(t)}{m_1} \tag{2.3}$$

Defining a new variable

$$w = x_2 - x_1 - l_0 \tag{2.4}$$

we obtain the following initial value problem

$$\begin{aligned} &\frac{d^2w}{dt^2} + \omega^2 w = -\frac{Ap_m}{m_1}\mathrm{e}^{-\frac{t}{t_m}} \qquad \omega^2 = k_s\Big(\frac{1}{m_1} + \frac{1}{m_2}\Big) \\ &w(0) = -\frac{m_2Ap_m}{(m_1+m_2)k_s} \qquad \frac{dw}{dt}\Big|_{t=0} = 0 \end{aligned} \tag{2.5}$$

The solution to the problem is given by

$$w(t) = -\frac{Ap_m}{m_1\omega^2(1+\omega^2t_m^2)}\Big[\omega t_m\sin(\omega t) + \cos(\omega t) + \omega^2t_m^2\mathrm{e}^{-\frac{t}{t_m}}\Big] \tag{2.6}$$

Making use of this, we obtain from the second equation of (2.2) an expression for acceleration of the forward part of the projectile

$$a(t) = \frac{Ap_m}{m(1+\omega^2t_m^2)}\Big[\omega t_m\sin(\omega t) + \cos(\omega t) + \omega^2t_m^2\mathrm{e}^{-\frac{t}{t_w}}\Big] \qquad m = m_1 + m_2 \tag{2.7}$$

Integrating (2.7) from 0 to t, we obtain the following formula for the velocity increase of the forward part of the projectile

$$\Delta u(t) = \frac{Ap_m t_m}{m(1+\omega^2 t_m^2)}\Big[1-\cos(\omega t)+\frac{1}{\omega t_m}\sin(\omega t)+\omega^2 t_m^2\Big(1-\mathrm{e}^{-\frac{t}{t_m}}\Big)\Big] \tag{2.8}$$

In model 2, the projectile is treated as an elastic cylindrical rod with the same caliber d and mass m as the real projectile and length $l_0 = 4m/(\pi d^2)$. The material properties of the rod are determined by its density ρ and Young's modulus E. It is assumed that the force $F_p(t)$ is produced by the pressure uniformly distributed at the left end of the rod. The pressure changes in time are described by (1.1). The loading produces a uniaxial stress state in the rod. It is assumed that there is no force at the right end of the rod. This assumption is justified by the observation that the pressure acting on the forward part of the projectile is much less than the pressure acting on its base in the whole phase when the projectile is accelerated. We assume that at the beginning of the process all parts of the rod have the same velocity and acceleration.

The mathematical model corresponding to physical model 2 is given by the following initial-boundary value problem in the Lagrangian coordinates

$$\begin{aligned}
&\rho u_{,t} = \sigma_{,x} \qquad && \sigma_{,t} = E u_{,x} \\
&u(x,0) = u_m \qquad && \sigma(x,0) = p_m\Big(\frac{x}{l_0}-1\Big) \\
&\sigma(0,t) = -p_m \mathrm{e}^{-\frac{t}{t_m}} \qquad && \sigma(l_0,t) = 0
\end{aligned} \tag{2.9}$$

Initial condition $(2.9)_{3,4}$ for the stress σ follows from the assumption that the whole rod has initially the same acceleration.

Solving the problem, we obtain the following expressions for the velocity increase and acceleration of the forward part of the projectile

$$\begin{aligned}
&\Delta u(t) = \Delta u_m\left[\frac{t}{T_w} - 2N + 2\sum_{j=1}^{N}\exp\Big(-\frac{t-(2j-1)T_w}{t_m}\Big)\right] \qquad && \Delta u_m = \frac{p_m}{\rho c} \\
&N = E\Big(\frac{n+1}{2}\Big) \qquad && n = 0,1,2,\ldots \qquad && T_w = \frac{l_0}{c} \qquad && c = \sqrt{\frac{E}{\rho}} \\
&a(t) = \Delta u_m\left[\frac{1}{T_w} - \frac{2}{t_m}\sum_{j=1}^{N}\exp\Big(-\frac{t-(2j-1)T_w}{t_m}\Big)\right]
\end{aligned} \tag{2.10}$$

2.2. Models of the shell

The physical object considered and its physical models are illustrated in Fig. 3. In model 3, the ogive and the base of the shell are treated as rigid masses. The wall of the shell of length l_0 is treated as an elastic hollow cylinder, whereas the filling (explosive) is treated as an elastic cylindrical rod with density ρ_f and velocity of sound c_f. It is assumed that there is no friction between the wall and the filling. Because the filling is more compressible than the wall, it can also be assumed that there is no contact between the filling and the ogive. A uniaxial stress state is assumed inside the wall and the filling.

The mathematical description of model 3 is given by the following initial-boundary value problem (the subscript f refers to the filling)

$$\begin{aligned}
&\rho u_{,t} = \sigma_{,x} \qquad && \sigma_{,t} = \rho c^2 u_{,x} \qquad && \rho_f u_{f,t} = \sigma_{f,x} \qquad && \sigma_{f,t} = \rho_f c_f^2 u_{f,x} \\
&u(x,0) = u_m \qquad && u_f(x,0) = u_m
\end{aligned} \tag{2.11}$$

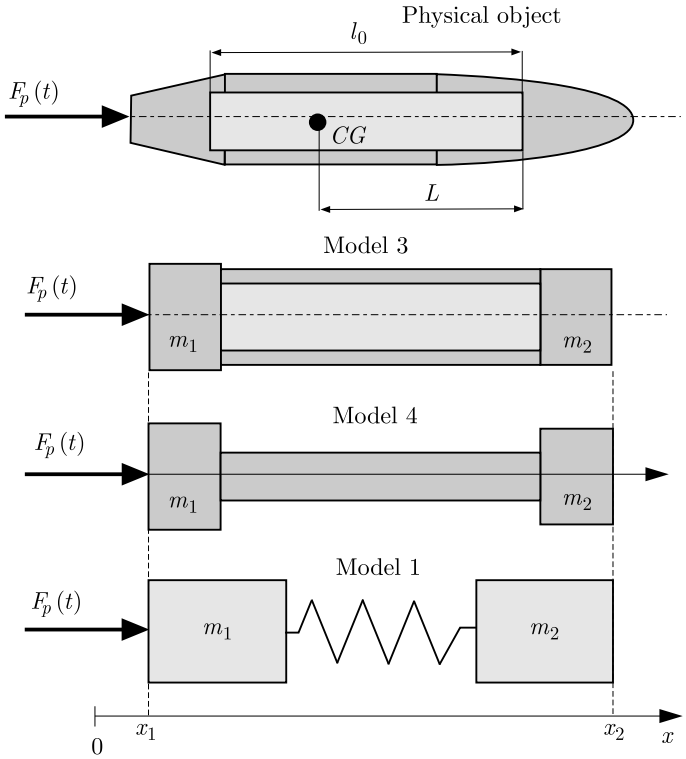

Fig. 3. Schemes of the physical object (a shell) and of models 1, 3 and 4 used for the analysis

and

$$\begin{aligned} &\sigma(x,0) = \rho a_0(x-l_0) - \frac{m_2 a_0}{A_c} \qquad a_0 = \frac{p_m A}{m_1 + m_2 + \rho l_0 A_c + \rho_f l_0 A_f} \\ &\sigma_f(x,0) = \frac{(m_1 + m_2 + A_c \rho l_0) a_0 - A p_m}{A_f} + \rho_f a_0 x \end{aligned} \tag{2.12}$$

and

$$\begin{aligned} &m_1 u_{,t}(0,t) = A p_m \mathrm{e}^{-\frac{t}{t_m}} + A_c \sigma(0,t) + A_f \sigma_f(0,t) \\ &m_2 u_{,t}(l_0,t) = -A_c \sigma(l_0,t) \qquad \sigma_f(l_0,t) = 0 \end{aligned} \tag{2.13}$$

where A_f, A_c mean the cross-sectional area of the filling and the wall.

The initial condition for stress (2.12) has been derived on the assumption that at the beginning of the process the whole shell has the same acceleration a_0 and on the assumption that there is no contact between the filling and the ogive. The second assumption has also been applied in the formulation of the boundary condition at $x = l_0$.

Problem (2.11)-(2.13) has been solved by the method of characteristics. The characteristic grid is shown in Fig. 4. It shows wave trajectories in the wall of the shell. The values of velocity and stress in the grid nodes are calculated using the characteristic relations

$$\Delta\sigma = \pm\rho c \Delta u \qquad \Delta x = \pm c \Delta t \qquad \Delta\sigma_f = \pm\rho_f c_f \Delta u_f \qquad \Delta x = \pm c_f \Delta t \tag{2.14}$$

In the node i, we have

$$\begin{aligned} &\sigma_i = \frac{\sigma_{i+1} + \sigma_{i-1} + \rho c(u_{i+1} - u_{i-1})}{2} \qquad u_i = u_{i-1} + \frac{\sigma_i - \sigma_{i-1}}{\rho c} \\ &\sigma_{fi} = \frac{\sigma_{fL} + \sigma_{fR} + \rho_f c_f (u_{fR} - u_{fL})}{2} \qquad u_{fi} = u_{fL} + \frac{\sigma_{fi} - \sigma_{fL}}{\rho_f c_f} \end{aligned} \tag{2.15}$$

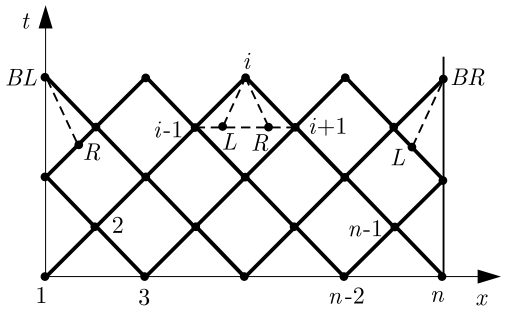

Fig. 4. Characteristic grid used for calculations for models 3, 4 and 5

The values of velocity and stress inside the filling in the auxiliary nodes L and R (characteristics $L-i$ and $R-i$ correspond to the wave velocity c_f) are calculated by a linear interpolation between the nodes $i-1$ and $i+1$

$$\begin{aligned} q_L &= q_{i-1} + (q_{i+1} - q_{i-1})\frac{c - c_f}{2c} \\ q_R &= q_{i-1} + (q_{i+1} - q_{i-1})\frac{c + c_f}{2c} \qquad q = \{u_f, \sigma_f\} \end{aligned} \tag{2.16}$$

The values of velocity and stress in nodes 1 and n are calculated by making use of an approximate form of boundary conditions (2.13) and relations at characteristics 1 – BL and n – BR

$$\begin{aligned} &u_{BL} = u_1 + a_1 \mathrm{e}^{-\frac{t}{t_m}}\left(1 - \mathrm{e}^{-\frac{2\Delta t}{t_m}}\right) + a_2(\sigma_1 + \sigma_{BL}) + a_3(\sigma_{f1} + \sigma_{fBL}) \\ &u_{fBL} = u_{BL} \qquad a_1 = \frac{A p_m t_m}{m_1} \qquad a_2 = \frac{A_c \Delta t}{m_1} \qquad a_3 = \frac{A_f \Delta t}{m_1} \\ &\sigma_{BL} = \sigma_2 - \rho c(u_B - u_2) \qquad \sigma_{fBL} = \sigma_{fR} - \rho_f c_f (u_{BL} - u_{fR}) \\ &u_{BR} = u_n - a_4(\sigma_n + \sigma_{BR}) \qquad a_4 = \frac{A_c \Delta t}{m_2} \qquad u_{fBR} = u_{fL} - \frac{\sigma_{fL}}{\rho_f c_f} \\ &\sigma_{BR} = \sigma_{n-1} + \rho c(u_{BR} - u_{n-1}) \qquad \sigma_{fBR} = 0 \end{aligned} \tag{2.17}$$

The values of velocity and stress inside the filling in the auxiliary nodes L and R are calculated by a linear interpolation between nodes 1-2 and $(n-1)$-n

$$q_L = q_n + (q_{n-1} - q_n)\frac{2c_f}{c + c_f} \qquad q_R = q_1 + (q_2 - q_1)\frac{2c_f}{c + c_f} \qquad q = \{u_f, \sigma_f\} \tag{2.18}$$

Calculations are performed in two iterations. In the first iteration, the values of stress are set as

$$\sigma_{BL} = \sigma_1 \qquad \sigma_{fBL} = \sigma_{f1} \qquad \sigma_{BR} = \sigma_n \tag{2.19}$$

In the second iteration, the values of stress calculated in the first iteration are used.

Neglecting friction between the wall and the filling is questionable because the filling is compressed and it exerts pressure on the wall. Instead of introducing the friction force into the model, two limiting cases are considered. The model without friction is the first limiting case. The second limiting case is a model for which it is assumed that the friction force is strong enough to exclude any displacement between the filling and the wall. If both models give similar results, it will be no necessity to take into account the friction force. In the second limiting case, the compressibility of the filling has no influence on the process. Its inertia can be taken

into account as an additional mass added to mass of the wall. This can be done by artificially increasing density of the wall material

$$\rho_a = \rho + \rho_f \frac{A_f}{A_c} \tag{2.20}$$

The central part of the shell can be treated as a cylindrical rod with cross-section area A_c and density ρ_a. This is the sense of model 4. Its mathematical form is not presented because it can be easily derived from problem (2.11)-(2.13) by neglecting all the expressions corresponding to the filling. Also the method of solving the problem is similar to that described for model 3.

In the modeling of the vibrations of the shell, model 1 can be used. The mass m_1 is calculated as the sum of mass of the base of the shell and mass of the wall and the filling lying between the base and the center of gravity. The mass m_2 is calculated as the sum of mass of the ogive and mass of the wall and the filling lying between the ogive and the center of gravity. The stiffness of the spring is calculated by using formula (2.1) with A replaced by A_c.

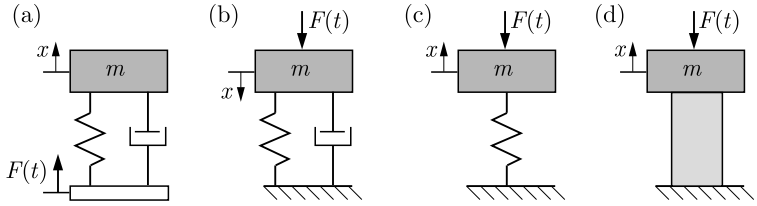

Fig. 5. Schemes of the model by Carlucci *et al.* (2013) (a), (b) and models 5 and 6 (c), (d)

In order to make comparison with the results of the model described by Carlucci *et al.* (2013), two more models are considered, as shown in Fig. 5. The vibrations are modeled in the reference frame moving with the center of gravity. Figure 5a shows the scheme of the model presented in Fig. 4 in the cited paper. It is erroneous because the force $F(t)$ should be applied to the mass m, not to the spring and the damper. It is the inertial force, so its value should be expressed as

$$F(t) = \frac{m}{m_s} F_p(t) \tag{2.21}$$

where m_s is the total mass of the shell. In Carlucci *et al.* (2013), the equality of both the forces was assumed. The proper form of the scheme is shown in Fig. 5b. The equations given in the cited paper correspond to this scheme. Figure 5c presents a scheme of model 5 considered in this work. It differs from the scheme in Fig. 5b by the absence of the damper and by the sign of the coordinate x. The mass m in model 5 is taken as the sum of mass of the ogive and 1/3 of mass of the shell wall. Figure 5d corresponds to model 6. The spring is replaced by an elastic rod with cross-section area A_c.

The mathematical model corresponding to model 5 is given by the following initial value problem

$$\begin{aligned} &m\frac{d^2w}{dt^2} + k_s w = -\frac{m}{m_s} A p_m \mathrm{e}^{-\frac{t}{t_m}} \qquad w = x - l_0 \\ &w(0) = -\frac{m}{m_s}\frac{A p_m}{k_s} \qquad \frac{dw}{dt}\Big|_{t=0} = 0 \end{aligned} \tag{2.22}$$

Solving this problem, the following expressions for the velocity increase and acceleration can be obtained

$$\begin{aligned} \Delta u(t) &= \frac{A m^2 p_m}{m_s(m + k_s t_m^2)}\Big[t_m \mathrm{e}^{-\frac{t}{t_m}} + t_m \sin(\omega t) - \frac{\omega}{k_s}\cos(\omega t)\Big] \\ a(t) &= \frac{A m^2 p_m}{m_s(m + k_s t_m^2)}\Big[\omega t_m \cos(\omega t) + \frac{\omega^2}{k_s}\cos(\omega t) - \mathrm{e}^{-\frac{t}{t_m}}\Big] \end{aligned} \tag{2.23}$$

The mathematical model corresponding to model 6 is given by the following initial-boundary value problem

$$\begin{aligned} &\rho u_{,t} = \sigma_{,x} \qquad \sigma_{,t} = \rho c^2 u_{,x} \qquad u(x,0) = u_m \qquad \sigma(x,0) = -\frac{mAp_m}{m_s A_c} \\ &u(0,t) = 0 \qquad m_2 u_{,t}\,(l_0,t) = -\frac{m}{m_s} Ap_m \mathrm{e}^{-\frac{t}{t_m}} - A_c \sigma(l_0,t) \end{aligned} \tag{2.24}$$

The problem is solved by the method of characteristics in the way described for model 3.

3. Results of the modeling

Calculations have been performed by making use of models 1 and 2 for a 30 mm gun used in the investigations presented by Leciejewski *et al.* (2012). The following values of parameters have been applied: $A = 7.07\,\mathrm{cm}^2$, $l_0 = 66\,\mathrm{mm}$, $m_1 = m_2 = 183\,\mathrm{g}$, $\rho = 7850\,\mathrm{kg/m}^3$, $E = 200\,\mathrm{GPa}$, $p_m = 51.5\,\mathrm{MPa}$, $t_m = 0.0211\,\mathrm{ms}$. The value of parameters p_m and t_m have been determined by the regression of the pressure course calculated by the model described in Trębiński and Czyżewska (2015). They are shown in Fig. 6. The dotted line corresponds to the approximation given by (1.2).

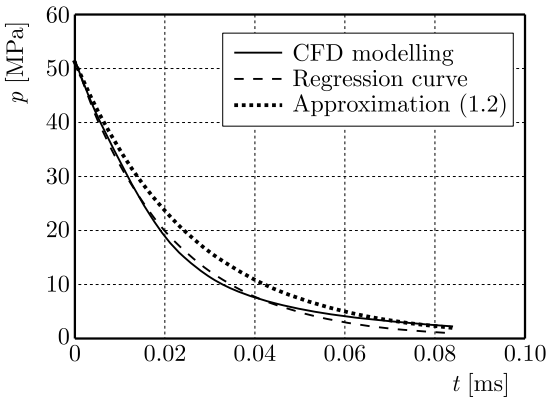

Fig. 6. Pressure course for a 30 mm gun calculated by the model proposed in Trębiński and Czyżewska (2015b), regression curve and approximation of the course using formulae (1.1) and (1.2)

Figures 7a and 7b present a comparison of the results obtained by models 1 and 2. Although the character of the velocity changes is different for the two models, the amplitude of oscillations is similar. It is much less than the amplitude of the velocity oscillations presented in Fig. 1. This suggests that these oscillations cannot be attributed to axial vibrations or wave reverberations in the projectile. We can suppose that these oscillations are caused by yawing of the projectile or by the effect of ionization of gases in strong shock waves arising in the vicinity of the muzzle (description of wave processes accompanying the exit of projectiles are given in Klingenberg and Heimerl (1988)).

As far as acceleration is concerned, the differences between the two models are much more pronounced. This means that it is recommended to take into account the wave motion in predicting the acceleration of a projectile leaving the muzzle.

Figures 8a and 8b present a comparison of the results obtained by models 5 and 6. The values of parameters used in calculations have been the same as in Carlucci *et al.* (2013): $A = 188\,\mathrm{cm}^2$, $A_c = 35\,\mathrm{cm}^2$, $l_0 = 508\,\mathrm{mm}$, $m = 3.75\,\mathrm{kg}$, $\rho = 7850\,\mathrm{kg/m}^3$, $E = 199\,\mathrm{GPa}$, $p_m = 68.9\,\mathrm{MPa}$, $t_m = 0.1731\,\mathrm{ms}$. For the purpose of comparison, it has been assumed that $m = m_s$. The two models give very close results. This means that in this case taking into account the wave reverberations is not necessary.

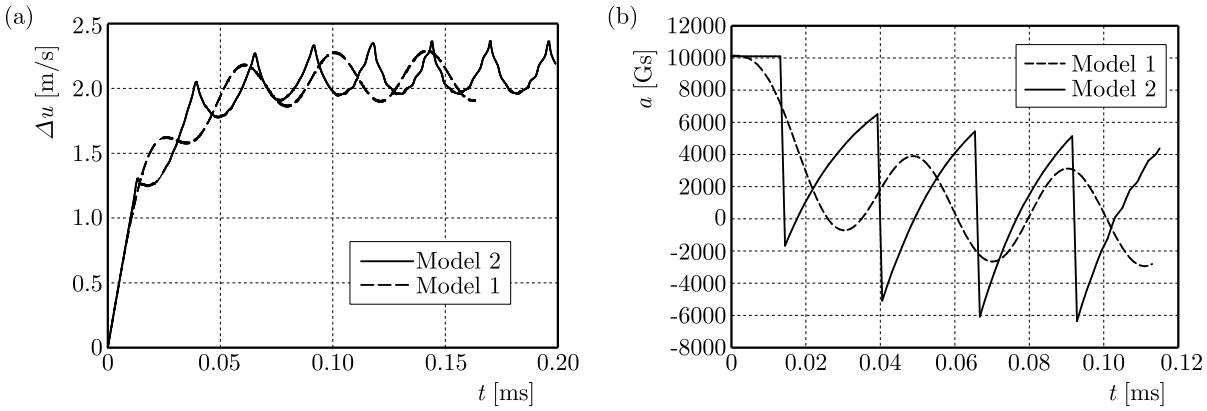

Fig. 7. Comparison of the (a) velocity increase and (b) acceleration courses calculated by the use of models 1 and 2

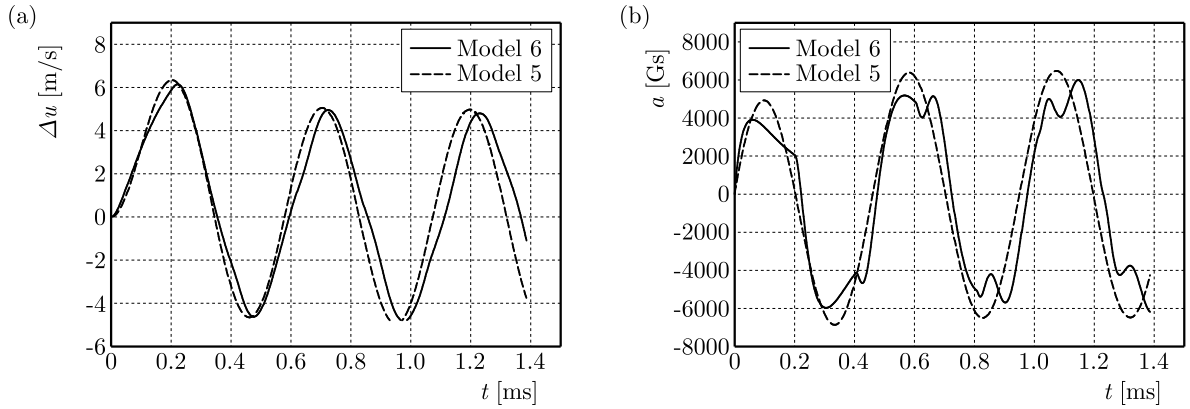

Fig. 8. Comparison of the (a) velocity increase and (b) acceleration courses of the shell ogive calculated by the use of models 5 and 6

The picture is somewhat different if we consider the wave motion in the whole shell. Figures 9a and 9b show a comparison of the calculated acceleration courses of the shell base and the shell ogive calculated by the use of models 3 and 4. The values of parameters applied in calculations have been as follows: $A = 188\,\mathrm{cm}^2$, $A_c = 93\,\mathrm{cm}^2$, $A_f = 95\,\mathrm{cm}^2$, $l_0 = 590\,\mathrm{mm}$, $m_1 = 6\,\mathrm{kg}$, $m_2 = 5\,\mathrm{kg}$, $\rho = 7850\,\mathrm{kg/m}^3$, $c = 5035\,\mathrm{m/s}$, $\rho_f = 1715\,\mathrm{kg/m}^3$, $c_f = 2470\,\mathrm{m/s}$, $p_m = 68.9\,\mathrm{MPa}$, $t_m = 0.1731\,\mathrm{ms}$.

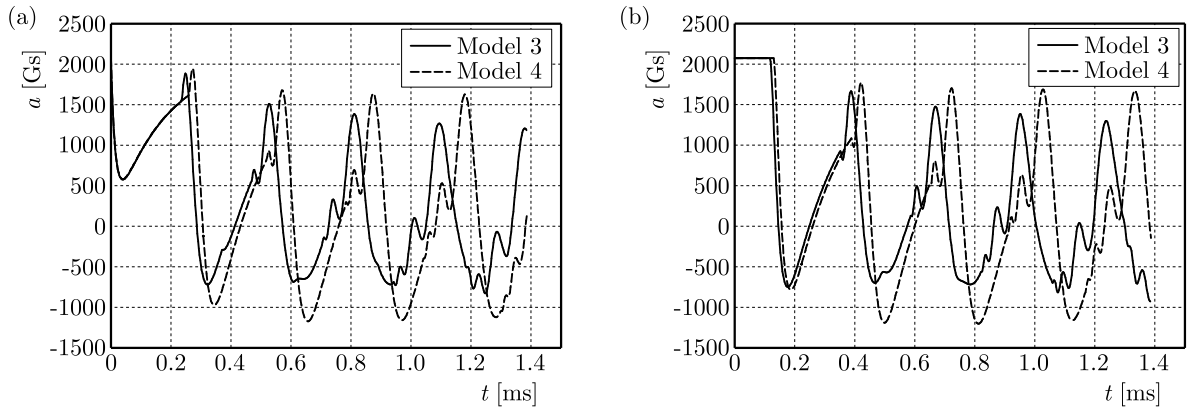

Fig. 9. Comparison of the (a) velocity increase and (b) acceleration courses of the shell ogive calculated by the use of models 3 and 4

Although models 3 and 4 represent the opposite limiting cases, as far as friction between the wall and the filling is concerned, they give close results. Therefore, simpler model 4 is recommended. The results obtained by making use of it are compared with the results from model 1 in Figs. 10a and 10b. Although the frequency of oscillations of the velocity and the acceleration values are very close, model 4 forecasts considerably larger amplitudes of oscillations.

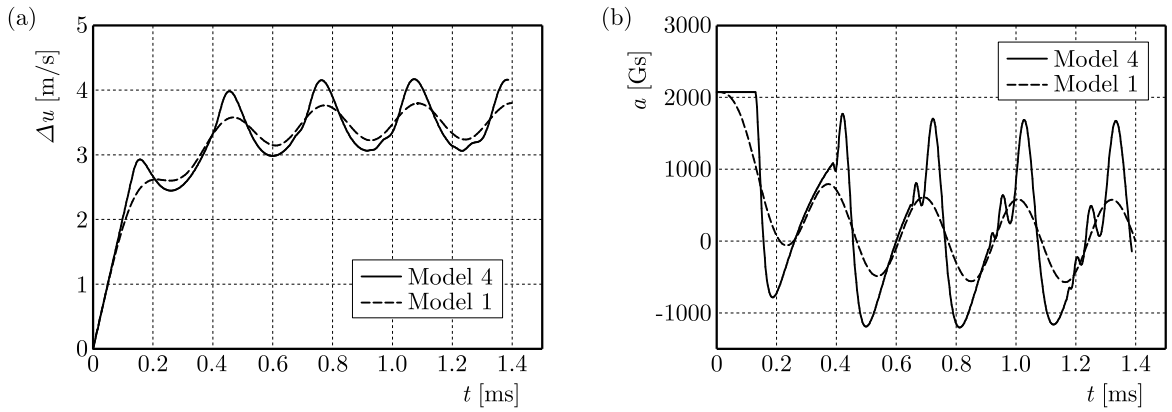

Fig. 10. Comparison of the (a) velocity increase and (b) acceleration courses of the shell ogive calculated by the use of models 4 and 1

Figure 11 presents the acceleration courses of the static center of gravity of the shell calculated by model 4. These are compared with the acceleration calculated for the shell treated as a rigid body. It can be seen that an accelerometer positioned in the static center of gravity will record acceleration courses that considerably differ from the mean acceleration of the shell.

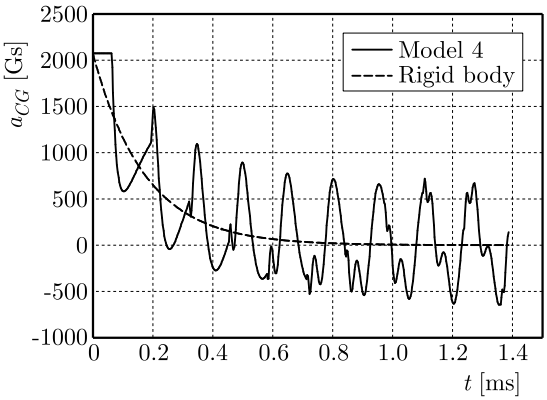

Fig. 11. Comparison of the acceleration courses of the shell static center of gravity calculated by the use of model 4 and for the shell treated as a rigid body

4. Conclusions

- Models taking into account wave reverberations generally predict similar frequencies and amplitudes of vibrations to the simple vibrational models. However, the character of time changes of acceleration differs considerably. Therefore, modeling of the wave motion is recommended for interpretation of the signals from accelerometers embedded in the shells.
- Close results obtained for models 3 and 4 prove it to be acceptable to assume that there is no displacement between the wall of the shell and the filling.
- The predicted amplitudes of velocity oscillations of the projectile leaving the muzzle are much smaller than those which can be deduced from the results of Doppler radar me-

asurements. Therefore, the observed oscillations of velocity cannot be solely attributed to vibrations of the projectile.

References

1. Carlucci D., Vega J., 2007, Empirical relationship for muzzle exit pressure in a 155 mm gun tube, [In:] *Computational Ballistics III*, C. A. Brebbia, edit., WIT Press, Ashurst, UK
2. Carlucci D.E., Frydman A.M, Cordes J.A., 2013, Mathematical description of projectile exit dynamics (set-forward), *ASME Journal of Applied Mechanics*, **80**, 031501-1
3. Klingenberg G., Heimerl J.M., 1988, *Gun Muzzle Blast and Flash*, **139**, AIAA Progress in Astronautics and Aeronautics edition
4. Leciejewski Z., Surma Z., Torecki S., Trębiński R., Czyżewska M., 2013, Theoretical and experimental investigations of projectile motion specifity in the intermediate period, *Proceedings of the 27th International Symposium on Ballistics*, Freiburg, Germany, 333-343
5. Trębinski R., Czyżewska M., 2015a, Approximate model of the intermediate ballistics, *Central European Journal of Energetic Materials*, **12**, 1, 77-88
6. Trębiński R., Czyżewska M., 2015b, Estimation of projectile velocity increase in the intermediate ballistics period, *Central European Journal of Energetic Materials*, **12**, 1, 63-76

Manuscript received January 5, 2015; accepted for print December 31, 2016